SherpaTT: A Versatile Hybrid Wheeled-Leg Rover

Florian Cordes[1] and Ajish Babu[1]

[1] DFKI Robotics Innovation Center Bremen, Germany
e-mail: *firstname.lastname@dfki.de*

Abstract

This paper subsumes the first experiences with the hardware of the robotic system SherpaTT. The mobile platform consists of four legs, each equipped with a wheel at its end. All legs are connected via a central body. The chosen control design and approach are validated with experiments using the robotic hardware. Autonomous active ground adaption is able to significantly improve the system's stability in terms of ground contact force tracking and body roll/pitch stability. For adaption, the robot makes use of a one dimensional force measurement per wheel and the roll and pitch angles as measured by an inertial measurement unit in the central body. The results of the experiments are an excellent base for further development of the motion capabilities of the rover.

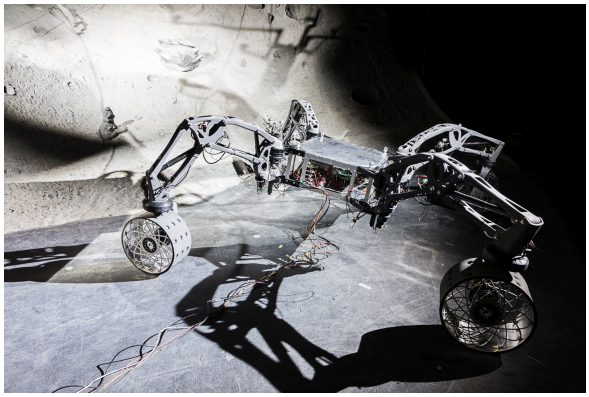

Figure 1. First integration stage of SherpaTT: four fully functional legs and a central body for locomotion mode development. Manipulator, high level sensors and protective hull are not mounted, yet.

1 Introduction

Mobile robots provide the possibility to collect data from remote locations and explore places that are too far away or too dangerous to be reached by humans. Since this implies that no humans are around once the robot is deployed, the robot needs to be self-sufficient, robust and possibly as autonomous as possible. Planetary exploration (currently primarily on Mars) is one example were mobile robots are deployed for exploration and gathering of scientific data.

From nature, walking and climbing seems to be the best solution for stable locomotion in a wide variety of terrains. Even though there are promising advancements in legged robotic locomotion [1, 9], the complexity and a persisting lack of robustness currently prevents these systems from being deployed in space missions.

As opposed to walking systems, wheeled robots offer a low complexity and high robustness. When equipped with appropriate suspension mechanisms these systems can provide a high mobility in natural terrain. So far, the mobile systems deployed on Moon (e.g. LRV [14], the Lunokhod rovers or Chang'e-3) and Mars (Pathfinder, MER [5], Curiosity [15]) are wheeled systems with passive suspension systems. The passive suspension known as rocker-bogie reduces the angular displacement the body of the robot is experiencing while traversing sloping terrain and allows to overcome obstacles such as rocks in the range of the wheel's diameter. A variation of the rocker-bogie is the triple bogie suspension with three independent rocker-arms that each interconnect two wheels of a six-wheeled rover [7, 8]. Another type of passive suspension system can be found in the rover CRAB [17], where three wheels on each side of the robot are connected via two links, creating a parallel bogie configuration. The mechanisms on each side of the rover are connected via a differential to level pitch angles of the body.

Hybrid systems with legs-on-wheels like presented in [3, 12] or wheels-on-legs as presented in [10, 13] provide a possibility to close the gap between walking and driving locomotion. A leg-on-wheel system imitates the movements of a walking system with a limited range of possible foot placements but vastly reduced kinematical complexity and often increased movement speed. On the other hand, wheel-on-leg (or wheeled-leg) systems are first and foremost driving systems. For adaption to sloping/rough terrain they need sensors, actuation and control algorithms. Depending on the design of the legs / the active suspension system, these systems provide the possibility to exhibit walking locomotion as well. Furthermore, active control of the central body's pose with respect to the

footprint in up to six degrees of freedom (DoF) is possible while simultaneously adapting to the terrain they are driving on.

This paper presents the first experiences with the hardware of the hybrid wheeled-leg system SherpaTT, which is depicted in Figure 1. The rover consists of four identical legs with a wheel at the end. For the experiments in this paper the first integration stage with fully functional legs mounted on the central body is used. In the final integration stage an additional manipulator will be mounted on top of the system. SherpaTT is part of a multi-robot team for an aspired lunar sample-return mission [11]. Following this introduction chapter, the second chapter gives an overview of the kinematics of the suspension system that is formed by the four legs, the third chapter highlights the motion control system implemented in SherpaTT.

2 SherpaTT: System Overview

In this section the general design of SherpaTT is presented. Currently, SherpaTT is in its first integration stage with all four leg units attached to a central body and the basic electronics implemented in the system for hardware testing (focus on the suspension system). The last paragraph of this section highlights some of the upcoming extensions of the system, that will be conducted to make SherpaTT a full member of the planned multi-robot system in the project TransTerrA [11]. SherpaTT is the successor of Sherpa, differences of both systems are highlighted in [4].

2.1 Leg Design and Definitions

As can be seen from Figure 1, SherpaTT features four leg-like units that constitute its active suspension system. A total of 20 active DoF distributed in four identical suspension units ("legs") are present.

For calculations of the kinematics, the Leg End Point (LEP) is defined as the point on a rigid wheel below the steering axis of that wheel as indicated in Figure 2. The LEP is used under the assumption of a rigid wheel on a rigid and flat surface. The LEP might be different from the Wheel Contact Point (WCP) which could be calculated using force/torque measurements [2] and the known stiffness of a flexible wheel. However, for the experiments and descriptions in this paper, we focus on the LEP as a first approximation.

The three DoF of each leg closest to the body (named *Pan*, *InnerLeg*, *OuterLeg*) are responsible for the movements of the LEP with respect to the body. The outermost DoF do not influence the LEP's position with respect to the body. These actuators rotate the wheel around its vertical axis (*WheelSteering*) and drive the wheel to create rolling motions of the robot (*WheelDrive*).

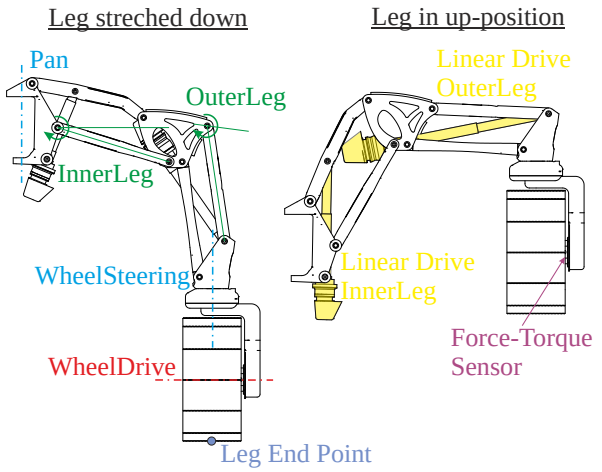

Figure 2. Degrees of Freedom of a Suspension Unit. Left: Configuration for high ground clearance, right: configuration with body on ground.

2.2 Leg Workspace

Figure 3 shows a cross-section of the toroid-shaped workspace built by the actual (still conservatively set) joint limits. Three preferred poses are indicated. These are LEP positions in the workspace, which provide maximum z-movement (up/down) for ground adaption (PrefPoseA), a compromise between radius movements and z-movementrange (PrefPoseB) and maximum body height (PrefPoseC). Note that the horizontal and vertical elements of the mock-up leg shown in the image keep horizontal/vertical due to the parallelogram structure used in the actual leg design.

The workspace is made up by moving the LEP towards or away from the body (changing the radius in the cylindrical leg coordinate frame, see also Section 3.1), moving the LEP up/down (z-component) and rotating around the pan joint.

A preferred pose is independent of the Pan joint position. Hence, different foot prints such as square, rectangular or any arbitrary four-sided polygon is possible. A preferred pose is used as standard commanded pose which is altered by offsets written from adaptive processes as described in Section 3.

2.3 Extensions of Current Integration State

Currently, SherpaTT is in an integration state, where the active suspension is put into operation while all other features of the system are still under development. A major mechanical upgrade is the mounting of the manipulator which was already used on the predecessor Sherpa [6]. The manipulator is used for payload-handling and optionally for locomotion support.

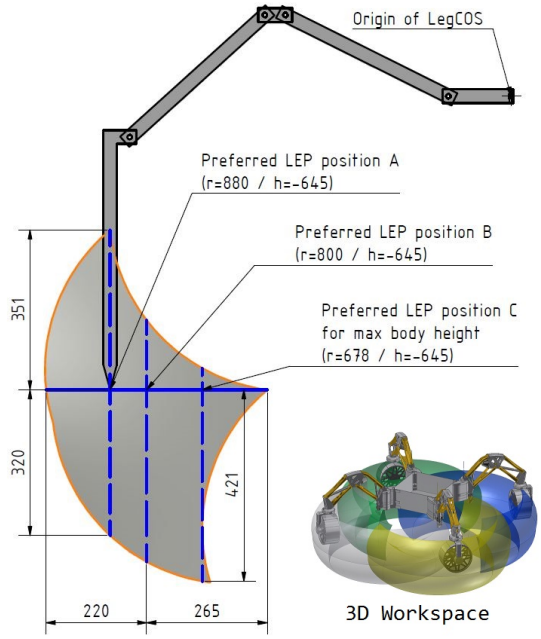

Figure 3. Workspace dimensions (cross section) and preferred poses in cylindrical leg frame. Inset depicts the overlapping workspaces of all four legs. Dimensions are in millimeters.

For a seamless integration into the multi-robot system [11], SherpaTT will be equipped with four payload interfaces (EMI: electro-mechanical interface [16]) around the manipulator tower and at the bottom of the body. The interfaces are used to transport payloads or to expand the rover's capabilities by attaching additional sensors and devices.

Finally a protective hull will be mounted on SherpaTT for protection against dust and other contaminants.

3 Motion Control

In this section, we present the motion control system (MCS) for SherpaTT. The MCS is the connecting layer between low-level control on one hand – i.e. firmware running on the hardware boards such as joint controllers, relay-boards and alike – and high level control (navigation, planning, and other autonomous behaviors) on the other. For the purpose of development of the MCS, a graphical user interface is used to command the robot's movement (forward, lateral and turn), its body attitude with respect to gravity (roll, pitch) and body height, and the footprint of the robot (where the LEPs of the suspension unit are with respect to the body). These are also

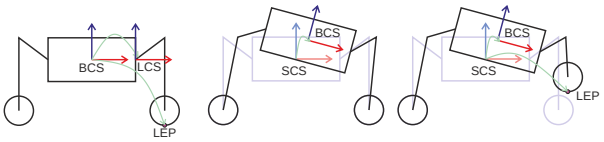

Figure 4. Coordinate Frames for Locomotion

the possible inputs for high-level processes to command the rover. Generation of joint commands from the mentioned high-level commands is completely encapsulated in the MCS.

3.1 Locomotion Coordinate Frames

Figure 4 illustrates the most important coordinate frames used in SherpaTT. The following main coordinate frames are used for locomotion control:

- The *Body Coordinate System* (BCS) is attached to the center of the main body of SherpaTT. Its z-axis is pointing upwards, the x-y plane is at the same height as the Leg Coordinate System's x-y plane (see below). This frame is used for all internal computations.
- The *Leg Coordinate System* (LCS) has its origin in the Pan joint of a leg. It is aligned with the Pan-CS when the Pan angle $\alpha = 0°$.
- The *Shadow Coordinate System* (SCS) is used to describe the motion commands independent of the body posture. The center image and the right hand image of Figure 4 illustrate the SCS. It is a virtual CS that remains at the "nominal pose" of SherpaTT. Body posture changes, externally commanded Leg End Point (LEP)-positions and movement commands are described in this frame.

3.2 Basic Structure of the Motion Control System

SherpaTT's *Motion Control System* (MCS) is setup to encapsulate the control of the robot's complex kinematics such that the high level process only needs to provide control inputs via a simple command interface. Figure 5 shows how the MCS is used to control the robot. In this simplified diagram the main command inputs are shown at the top:

- The *Motion Command* is used for basic robot movement. The command is three dimensional and allows commanding forward (x) and lateral (y) as well as turn movements (about z).
- *BodyPosture* commands are used to control the six DoF of the robot's main body.
- A *FootPrint* command is used to describe the three DoF of each LEP.

This results in a total of 21 possible command inputs. Three of which are velocity commands, the rest are

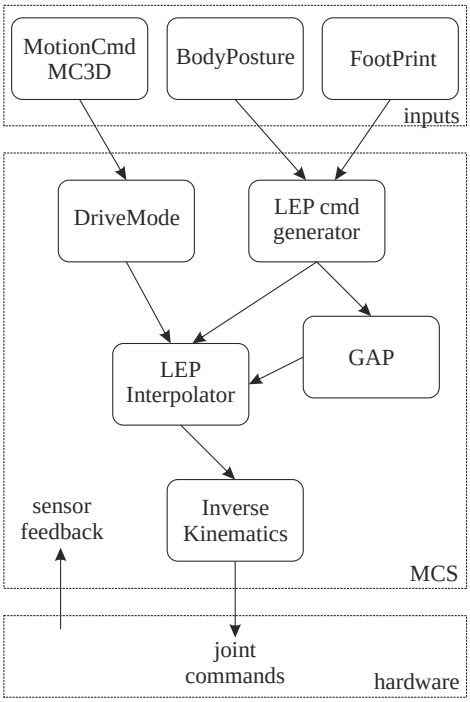

Figure 5. Simplified structure of SherpaTT's Motion Control System. Only central components are displayed.

position commands. Note that height commands (z-component) for single LEPs can be set freely, however these commands have an influence on the BodyPosture. Hence, even if possible in the actual MCS implementation, direct z-commands for the LEPs should be avoided by the human operator or the high-level processes.

Internally, the BodyPosture command and the FootPrint command are merged into one LEP position (in BCS) per leg of the suspension system. The MotionCommand is used to control the WheelSteering and WheelDrive joints according to the DriveMode. The commanded values are merged together with LEP offsets originating from the *Ground Adaption Process* (GAP, see Section 3.3) into the LEP Interpolator. Here the trajectories of the LEP positions are generated to reach a new desired LEP from the actual LEP position.

In each cycle of the MCS (which is executed at 100 Hz), the actual LEP command is finally converted into joint commands by the Inverse Kinematics task and sent to the joints of the suspension system. The sensor feedback contains telemetry from each joint as well as IMU data for the actual body orientation and data from the force-torque sensors at each wheel.

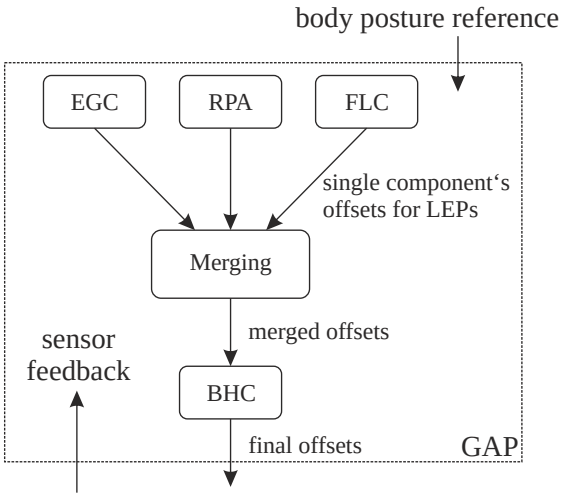

Figure 6. The components of the Ground Adaption Process (GAP): Ensure Ground Contact (EGC), Roll/Pitch Adaption (RPA), Force Leveling Control (FLC), and Body Height Correction (BHC).

3.3 Active Ground Adaption

The Ground Adaption Process (GAP) is the part of the MCS that manipulates the LEPs of each leg to conform to the terrain. This is achieved by following reference values for forces at the LEP and roll and pitch angle of the central body as measured by the Inertial Measuring Unit (IMU). The reference values are tracked using PI-controllers for each of the setpoint goals. Figure 6 displays the general scheme in which the values for active ground adaption are generated.

Currently, three subcomponents constitute the ground adaption. The three offset generating subcomponents of GAP are described in more detail in the following paragraphs. Each of the components independently calculates an LEP offset (in z-direction) for each of the wheels. The offsets are then merged into one offset for each wheel. Before writing the merged offsets out to the MCS, the *Body Height Control (BHC)* module checks whether all offsets have the same sign, when this is the case, the offsets are cut such that the smallest offset is set to zero. Hence, a body height drift can be prevented.

Ensure Ground Contact (EGC) This module is responsible for keeping all wheels in continuous ground contact. Once the measured force on a wheel drops below a threshold, the corresponding wheel offset is adapted such that the wheel moves down with $\dot{z}_{LEP,i} = -10\,mm/s$.

Roll/Pitch Adaption (RPA) In the RPA subcomponent, two separate PI controllers are active for each wheel's offset, resulting in eight PI-controllers in total. One controller generates offsets to match the commanded roll, the second controller to match the commanded pitch angle of the body. In the implementation used for the experiments presented in this paper, both controllers assume a distance of the wheel to the rotation axis of 1 m. An extension to arbitrary foot prints is possible by incorporating the x and y component of the LEP in body coordinates as scaling factor. Both offsets of the RPA module are added and written as combined RPA offset.

Force Leveling Control (FLC) The force leveling module needs the expected forces at the wheels as input for the PI controller. Currently, the forces are calculated as expected forces for the footprint the robot is driving. In other words, when driving in a symmetrical square foot print configuration, each wheel is expected to share the same fraction of the robot's mass. Wheels that are closer to the body would share a higher load. Since the system with four ground contact points is underdetermined, an approximation using a Moore-Penrose pseudoinverse is used to generate the reference forces for the wheels. For this static equilibrium is assumed. In later development stages, other ground adaption modules will actively change the position of the center of gravity within the support polygon to generate an appropriate force distribution between the wheels for locomotion in rough and sloping terrain.

4 Experiments

For validating the systems's ground adaption capabilities, experiments on a wooden obstacle track are conducted. The initial experiments using the first integration study of SherpaTT and the results thereof are presented in this section.

4.1 Setup

Figure 7 shows the experimental setup. An obstacle with two up-down slopes of 20 cm height is used. During the experiment the rover is commanded in such a way, that it drives "one-sided" over the obstacle with its left wheels, while the wheels front-right (FR) and rear-right (RR) roll over flat laboratory floor. In the chosen foot print of the robot each wheel contact point is in the corner of a square with an edge length of $\sim 2\,m$. Hence, during most of the run only one wheel is on the obstacle; when the front wheel is about to drive off the obstacle, the rear wheel has just been driven onto the first slope.

All experiments use a constant forward velocity of $\dot{x} = 50\,mm/s$ and a symmetrical, square-shaped footprint. Each wheel is approximately at a distance of 1 m from

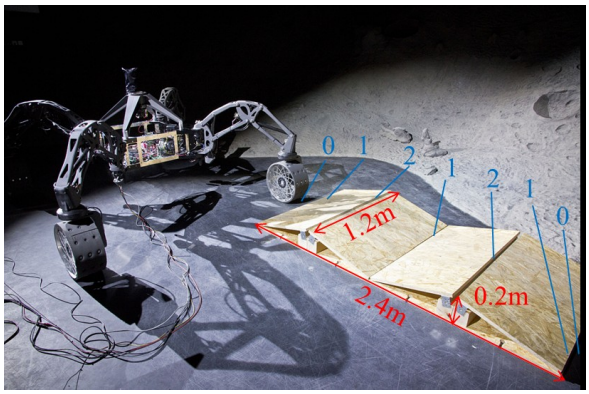

Figure 7. Obstacle track with dimensions as used for the presented experiments. Blue digits identify the experiment markers for the wheel position in the log data stream. Note that during the experiments the manipulator flange was already mounted on SherpaTT.

the rover's roll and pitch axis, respectively. For reference, the experiment is conducted without ground adaption, i.e. with a stiff suspension system, and then compared with the data using active ground adaption. During the run, experiment markers are set manually for the position of the front-left (FL) and rear-left (RL) wheel on the obstacle: A marker value of "0" indicates a wheel on laboratory floor, changing the value to "1" marks the beginning of an upslope, while setting the marker to "2" indicates the beginning of a down-slope. The experiment markers are shown in Figure 7 as blue digits at the point where they are set.

In the data plots of Figure 8 and Figure 9, the experiment markers are shown for the front left and rear left wheel as light blue and yellow line, respectively. Please note that due to the manual setting, the markers are not precisely set. However, orientation in the data is more easy with these markers. Furthermore, in between the run without adaption and the run with active adaption, the manipulator flange was mounted on the rover. This is reflected in the slightly higher overall weight of the rover ($F_{g1} \approx 1200\,N$ in the run without adaption vs. $F_{g2} \approx 1400\,N$ in the run with active ground adaption).

All presented plots are single-run data. Comparison of different runs showed a high repeatability, with in only marginal differences between the single runs.

4.2 Results

Figure 8(a) shows the roll and pitch data from a run without active adaption of the suspension system. The roll angle is more or less constant at around 1°, once a wheel is on the obstacle (blue line). A peak of about 3° in roll is visible when wheel FL is still on the last slope and wheel

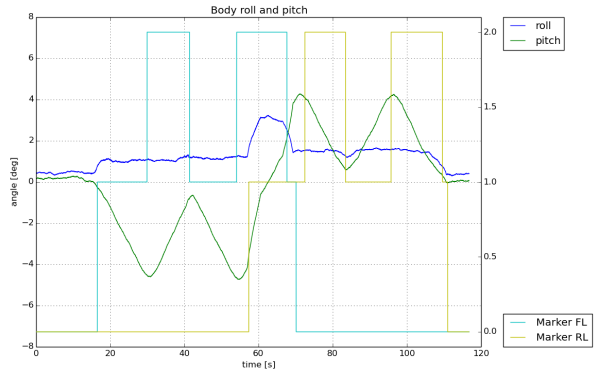

(a) Without adaption, the obstacle-course is well visible in the pitch of the robot.

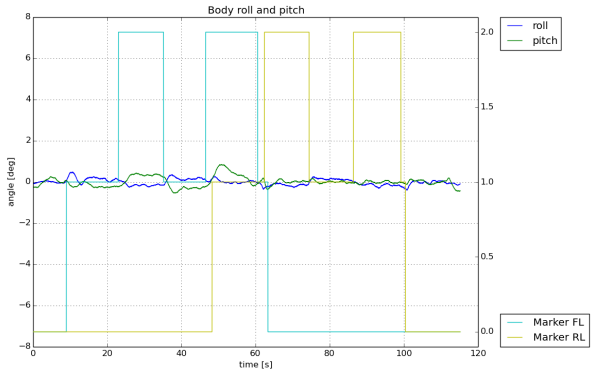

(b) Active adaption limits the values within ±1deg max

Figure 8. Roll/Pitch deviation without and with active GAP.

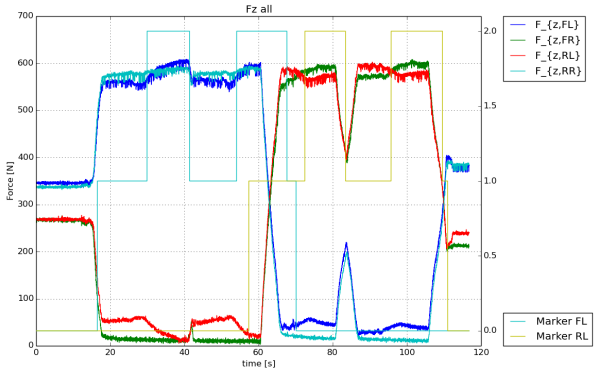

(a) Without adaption, wheels loose ground contact (F_z ≈0 N). Two diagonally opposite wheels (FL/RR and FR/RL) share the main load of the robot's weight.

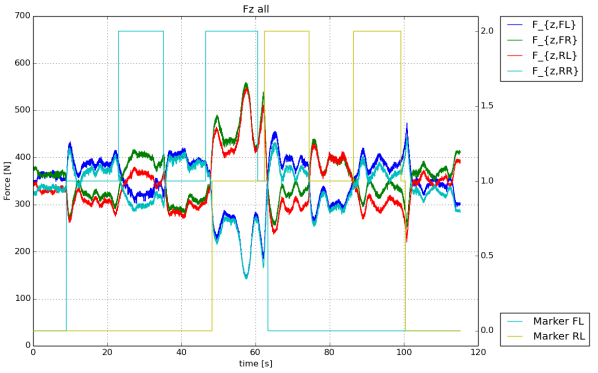

(b) Active adaption limits the values mostly to ±100 N of the desired value (≈300 N). A higher deviation is visible in the middle of the experiment, where the rear wheel enters the obstacle while the front wheel leaves the obstacle

Figure 9. Wheel-ground contact forces without and with active GAP.

RL drives up the first slope (around $t = 60\,s$).

In the pitch data of the rover, the obstacle is quite well recognizable, with a negative pitch following the two peaks of the obstacle when the FL wheel is on the obstacle and a positive pitch, when the rear wheel is on the obstacle. From the corresponding force plot in Figure 9(a) it can be seen that the wheels FR and RR loose ground contact (z-force drops close to zero).

The force plot also shows that with the stiff suspension there are always two *strong contacts* and two *weak contacts*. Both types are diagonally opposed to each other, i.e. FL/RR and FR/RL are contact pairs. The robot is driving with a symmetrical foot print. With a weight of $F_{g1} \approx 1200\,N$, each wheel contact should ideally remain at around $300\,N$. Actually, due to the stiff suspension and the resulting lift off the ground of single wheels, the forces deviate about $\pm 300\,N$ from the desired reference force.

Figure 8(b) and Figure 9(b) show the results of driving over the same obstacle with active GAP. With active control of roll and pitch angles both are kept within ±0.5°, apart from one deviation of about 1° around 50 s (ref. Figure 8(b)). In the second half of the experiment (RL wheel on obstacle) the angles are kept within ±0.2°.

From the plot of the wheel contact forces, it can be seen that all wheels keep ground contact during the complete experiment run. Control oscillations lead to more frequent switching between strong and weak contact pairs. The oscillations are a result of a limited velocity of the wheel's z-component, which is due to the single joint velocity limits in each leg. Apart from greater force deviations during the change over of FL and RL wheel on the obstacle, the force levels are kept approximately $\pm 50\,N$

around the setpoint of $\frac{1}{4}F_{g2} = 350\,N$.

5 Conclusion and Outlook

This paper gives a first impression of the newly integrated hybrid driving and walking rover SherpaTT.

The structure and kinematics of the suspension system are highlighted, and the implemented control system is presented. Core part of the motion control system is the active ground adaption process (GAP). This process is implemented in such a way that offsets to the commanded wheel position are written to adapt to sloping terrain. Measurement inputs are currently one-dimensional force measurements at the wheels and orientation measurements (roll/pitch) in the central body.

The initial experiments presented in this paper show that a clear reduction in loads of a single wheel by active force balancing is possible. The deviation of forces was reduced to $\pm 50\,N$ as opposed to deviations of $\pm 300\,N$ in case of no adaption to the obstacle. The implemented roll and pitch controller is able to keep the body's pose close to the desired values ($\pm 0.5°$ vs. $\pm 4.5°$ without active adaption) on the obstacle used for the experiments, significantly reducing the ground's effect onto the body's orientation. In the presented experiments, rough control gain setting was done, it is to be expected that tuning of control parameters will improve the oscillating behavior and reference value tracking. A high repeatability was observed, differences between single runs with same settings are only marginal.

Even though the experiments in this paper indicate a good behavior of the robot concerning the active adaption to sloping terrain, only a limited subset of system configurations was investigated so far. Further developments are currently directed into arbitrary foot prints (non-symmetric stance and LEPs in other distances than 1 m from rotation axis), three dimensional force tracking and LEP offset generation, and less regular as well as bigger obstacles.

Acknowledgment

The project TransTerrA is funded by the German Space Agency (DLR, Grant number: 50RA1301) with federal funds of the Federal Ministry of Economics and Technology (BMWi) in accordance with the parliamentary resolution of the German Parliament.

References

[1] S. Bartsch. "Development, Control, and Empirical Evaluation of the Six-Legged Robot SpaceClimber Designed for Extraterrestrial Crater Exploration". In: *KI - Künstliche Intelligenz* 28.2 (2014), pp. 127–131. URL: http://dx.doi.org/10.1007/s13218-014-0299-y.

[2] A. Bicchi, J. K. Salisbury, and D. L. Brock. *Contact Sensing from Force Measurements*. A.I. Memo No. 1262. Massechusetts Institute of Technology, Artificial Intelligence Laboratory, 1990, pp. 249–262. URL: ftp://publications.ai.mit.edu/ai-publications/pdf/AIM-1262.pdf.

[3] Y. C. Chou et al. "Bio-inspired step crossing algorithm for a hexapod robot". In: *Intelligent Robots and Systems (IROS), 2011 IEEE/RSJ International Conference on*. 2011, pp. 1493–1498.

[4] F. Cordes et al. "An Active Suspension System for a Planetary Rover". In: *Proceedings of the International Symposium on Artificial Intelligence, Robotics and Automation in Space (i-SAIRAS 2014); June 17-19, Montreal, Canada*. o.A., June 2014.

[5] R.A. Lindemann and C.J. Voorhees. "Mars Exploration Rover mobility assembly design, test and performance". In: *Systems, Man and Cybernetics, 2005 IEEE International Conference on*. Vol. 1. 2005, 450–455 Vol. 1.

[6] M. Manz et al. "Development of a Lightweight Manipulator Arm using Heterogeneous Materials and Manufacturing Technologies". In: *Proceedings of the International Symposium on Artificial Intelligence, Robotics and Automation in Space (i-SAIRAS 2012); September 4-6, Turin, Italy*. o.A., Sept. 2012.

[7] Paul Meacham, Nuno Silva, and Richard Lancaster. "The Development of the Locomotion Performance Model (LPM) for the ExoMars Rover Vehicle". In: *Proceedings of ASTRA 2013*. 2013. URL: http://robotics.estec.esa.int/ASTRA/Astra2013/Papers/meacham_2811294.pdf.

[8] S. Michaud et al. "Development of the ExoMars Chassis and Locomotion Subsystem". In: *Proceedings of i-SAIRAS 2008 - 9th International Symposium on Artificial Intelligence, Robotics and Automation in Space*. 2008. URL: http://elib.dlr.de/55365/1/i-sairas2008_ExoMars.pdf.

[9] M. Raibert et al. *BigDog, the Rough-Terrain Quadruped Robot*. online. 2008. URL: http://www.bostondynamics.com/img/BigDog_IFAC_Apr-8-2008.pdf.

[10] W. Reid, A. H. Göktogan, and S. Sukkarieh. "Moving MAMMOTH: Stable Motion for a Reconfigurable Wheel-On-Leg Rover". In: *Proceedings of Australasian Conference on Robotics and Automation*. 2014.

[11] R. Sonsalla et al. “Towards a Heterogeneous Modular Robotic Team in a Logistic Chain for Extraterrestrial Exploration”. In: *Proceedings of the International Symposium on Artificial Intelligence, Robotics and Automation in Space (i-SAIRAS 2014); June 17-19, Montreal, Canada*. o.A., June 2014.

[12] R. U. Sonsalla et al. “Design of a High Mobile Micro Rover within a Dual Rover Configuration for Autonomous Operations”. In: *Proceedings of the International Symposium on Artificial Intelligence, Robotics and Automation in Space (iSAIRAS-2014)*. Montreal, 2014.

[13] J. Townsend, J. Biesiadecki, and C. Collins. “ATHLETE mobility performance with active terrain compliance”. In: *Aerospace Conference, 2010 IEEE*. 2010, pp. 1–7.

[14] NASA Webpage. *The Apollo Lunar Roving Vehicle*. `http://nssdc.gsfc.nasa.gov/planetary/lunar/apollo_lrv.html`. last visit: 2016-02-09.

[15] R. Welch et al. “Verification and validation of Mars Science Laboratory surface system”. In: *System of Systems Engineering (SoSE), 2013 8th International Conference on*. 2013, pp. 64–69. URL: `http://ieeexplore.ieee.org/xpl/articleDetails.jsp?arnumber=6575244&queryText=Verification%20and%20Validation%20of%20the%20MSL%20Curiosity%20Rover&newsearch=true`.

[16] W. Wenzel, F. Cordes, and F. Kirchner. “A Robust Electro-Mechanical Interface for Cooperating Heterogeneous Multi-Robot Teams”. In: *Proceedings of the 2015 IEEE International Conference on Intelligent Robots and Systems (IROS-15)*. Hamburg, 2015, pp. 1732–1737.

[17] B. Xu et al. “Composite control based on optimal torque control and adaptive Kriging control for the CRAB rover”. In: *Robotics and Automation (ICRA), 2011 IEEE International Conference on*. 2011, pp. 1752–1757.